Revista Española de Enfermedades Digestivas
The Spanish Journal of Gastroenterology

**Title:**
**In vitro characterisation of the SETD8-MCM7 axis in driving gastric cancer progression and epithelial-mesenchymal transition**

Authors:
Chuanxia Zhang, Yang Zhang, Mengyuan Kang, Heng Lu, Xiaoxi Wan

DOI: 10.17235/reed.2026.11700/2025
Link: PubMed (Epub ahead of print)

Please cite this article as:
Zhang Chuanxia, Zhang Yang, Kang Mengyuan, Lu Heng, Wan Xiaoxi. In vitro characterisation of the SETD8-MCM7 axis in driving gastric cancer progression and epithelial-mesenchymal transition. Rev Esp Enferm Dig 2026. doi: 10.17235/reed.2026.11700/2025.

Revista Española de Enfermedades Digestivas
The Spanish Journal of Gastroenterology

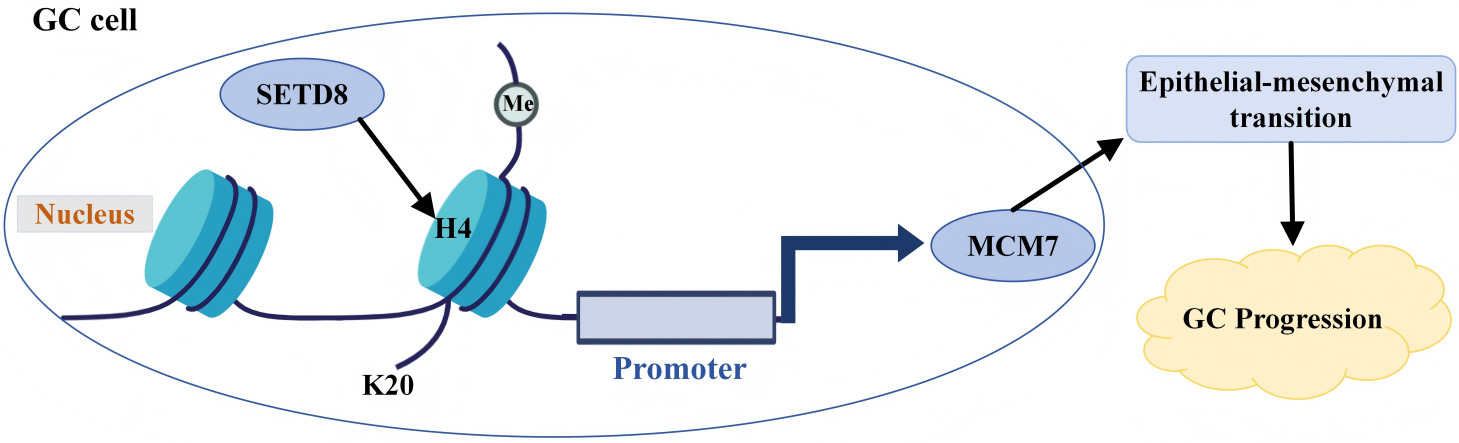

Revista Española de Enfermedades Digestivas
The Spanish Journal of Gastroenterology

# *In vitro* characterisation of the *SETD8-MCM7* axis in driving gastric cancer progression and epithelial-mesenchymal transition

Chuanxia Zhang[#], Yang Zhang[#], Mengyuan Kang, Heng Lu, Xiaoxi Wan[*]

Department of Oncology, Shanghai Pudong New Area People's Hospital, Shanghai, 200120, China.

**#These authors are listed as co-first authors.**

***Corresponding author information**

Xiaoxi Wan, Department of Oncology, Shanghai Pudong New Area People's Hospital; No. 490, Chuanhuan South Road, Shanghai 200120, China.

Email: wanxiaoxi@shpdph.com

**Authors' contributions**

(I) Conception and design: C Zhang, Y Zhang
(II) Administrative support: C Zhang, M Kang
(III) Provision of study materials: H Lu, X Wan
(IV) Collection and assembly of data: Y Zhang, H Lu
(V) Data analysis and interpretation: C Zhang, Y Zhang, X Wan
(VI) Manuscript writing: All authors.
(VII) Final approval of manuscript: All authors.

Revista Española de Enfermedades Digestivas
The Spanish Journal of Gastroenterology

## Highlights

1. *SETD8* is upregulated in gastric cancer (GC) and promotes malignant phenotypes in vitro, including proliferation, migration, invasion, and stemness.

2. *SETD8* facilitates epithelial-mesenchymal transition (EMT) and cancer progression by upregulating *MCM7* expression, potentially through an H4K20me1-dependent epigenetic mechanism.

3. MCM7 serves as a critical functional downstream effector, as its overexpression partially rescues the phenotypic suppression caused by *SETD8* knockdown.

4. The *SETD8*/MCM7 axis is correlated with advanced clinical stages and represents a promising therapeutic target in GC.

## Abstract

**Background:** SETD8, a histone methyltransferase catalyzing H4K20 monomethylation (H4K20me1), is crucial for epigenetic regulation, yet its role in gastric cancer (GC) progression remains unclear. This study investigated whether SETD8 promotes epithelial-mesenchymal transition (EMT) and GC progression by regulating *MCM7*.

**Methods:** expression and clinical relevance of *SETD8* and *MCM7* were analyzed using TCGA and GEO databases, and validated in GC cell lines and normal gastric epithelial cells. *SETD8* knockdown and inhibitor UNC0379 were used to assess its functions. Proliferation, apoptosis, invasion, migration, EMT and stemness were evaluated by CCK-8, flow cytometry, Transwell, wound healing, immunofluorescence and sphere formation assays. ChIP-qPCR measured H4K20me1 enrichment and SETD8 binding at the *MCM7* promoter. Rescue experiments were performed by overexpressing *MCM7* in SETD8-knockdown cells. Supplementary single-cell and immunotherapy cohort analyses were also conducted.

**Results:** *SETD8* and *MCM7* were overexpressed in GC tissues and cell lines, correlating with advanced stage and poor prognosis. *SETD8* knockdown suppressed proliferation, migration, invasion and stemness, induced apoptosis, and reversed EMT (downregulating Snail, N-cadherin, Vimentin; upregulating E-cadherin). Mechanistically, *SETD8* knockdown reduced global H4K20me1

Revista Española de Enfermedades Digestivas
The Spanish Journal of Gastroenterology

and *MCM7* expression. H4K20me1 was enriched at the *MCM7* promoter, while direct SETD8 binding was not detected, suggesting a non-canonical regulatory mode. *MCM7* overexpression rescued the malignant phenotypes inhibited by *SETD8* knockdown.

**Conclusion:** SETD8 promotes EMT and GC progression primarily by upregulating *MCM7* expression, likely via an H4K20me1-dependent epigenetic mechanism. MCM7 acts as a key downstream effector. The *SETD8*/MCM7 axis represents a novel driver and potential therapeutic target in GC.

**Keywords**: Gastric cancer. Epithelial-mesenchymal transition. *SETD8*/*MCM7*. Histone H4 lysine 20 monomethylation (H4K20me1).

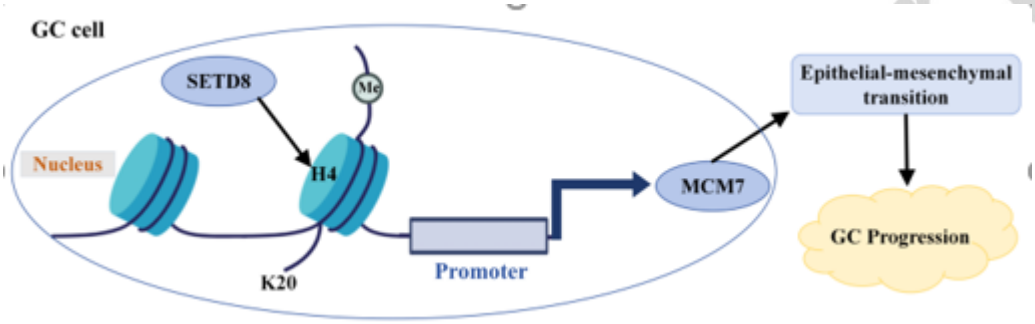


**Graphical Abstract**. *SETD8* Drives Gastric Cancer Metastasis via H4K20me1-*MCM7*-EMT Axis. Histone methyltransferase *SETD8* upregulates the expression of *MCM7* by catalyzing the H4K20me1 modification, thereby driving epithelial-mesenchymal transition and promoting the progression of gastric cancer.

## 1. Introduction

Gastric cancer (GC) is one of the most prevalent and lethal malignancies worldwide. Statistics indicate that the five-year survival rate of GC remains low, primarily due to its highly invasive nature and early metastatic potential [1, 2]. Epithelial-mesenchymal transition (EMT) is a crucial biological process that endows epithelial cells with mesenchymal-like characteristics, thereby enhancing their migratory and invasive capabilities [3]. During GC progression, EMT is considered a

key mechanism driving distant metastasis [4]. Therefore, elucidating its regulatory mechanisms is essential for identifying potential therapeutic targets.

Although the role of EMT in GC progression has been extensively studied, the upstream epigenetic regulatory mechanisms governing EMT remain largely unexplored, particularly the dynamic regulation of EMT-related genes by histone modifications. SET domain containing 8 (SETD8) is a methyltransferase that specifically catalyzes monomethylation of histone H4 at lysine 20 (H4K20me1), playing a pivotal role in chromatin remodeling, DNA damage repair, and cell cycle regulation [5]. Emerging evidence suggests that *SETD8* is aberrantly expressed in various malignancies and influences tumor progression by modulating transcription factors, non-coding RNAs, and epigenetic modifications [6-8]. For instance, in breast cancer [9, 10] and endometrial cancer [11], SETD8 facilitates transcriptional activation of key genes through H4K20me1 modifications, thereby promoting cellular proliferation and migration. However, the functional role of *SETD8* in GC and its relationship with EMT remain unclear. Notably, H4K20me1 is frequently enriched at gene promoter regions, potentially influencing transcription factor binding by modulating chromatin accessibility.

Recent studies have identified MCM7, a highly conserved minichromosome maintenance protein, as a key regulator of tumor progression [12]. *MCM7* is aberrantly activated in various solid tumors and is associated with tumor cell proliferation, invasion, metastasis, and drug resistance [13, 14]. Mechanistically, MCM7 regulates multiple oncogenic signaling pathways, such as PI3K/AKT [14] and Wnt [15, 16], both of which contribute to cancer cell growth and EMT induction [17]. In GC, *MCM7* overexpression has been strongly correlated with tumor malignancy and progression [18, 19]. However, whether *MCM7* expression is regulated by epigenetic mechanisms remains unknown. Bioinformatics analysis revealed a co-expression pattern between *SETD8* and *MCM7* in GC tissues, suggesting a potential functional link between the two. Moreover, H4K20me1 modification may regulate *MCM7* promoter activity, thereby modulating its transcription and promoting EMT. Nevertheless, this hypothesis requires further experimental validation.

Based on these findings, we propose that *SETD8* may promote GC progression through *MCM7* upregulation and EMT induction. This study aims to explore the role of *SETD8* in GC using bioinformatics and in vitro models, and to investigate whether its effects are mediated through *MCM7*.

Revista Española de Enfermedades Digestivas
The Spanish Journal of Gastroenterology

## 2. Methods：

### 2.1 Dataset analyses

The RNA expression data and clinical information were retrieved from The Cancer Genome Atlas (TCGA) database (https://www.cancer.gov/tcga)（Normal:36, Tumor:412. The transcriptomic data (TPM, Transcripts Per Million) downloaded from UCSC were utilized for a comprehensive pan-cancer analysis. TIMER2.0 (https://compbio.cn/timer2/) is a comprehensive resource repository that enables systematic analysis of immune infiltration across diverse cancer types, , thereby facilitating an in-depth exploration of tumor immunological, clinical and genomic characteristics. Single-cell transcriptomic data of gastric cancer were obtained from the GSE183904 dataset, bulk transcriptomic and data from the GSE15459 dataset, and immunotherapy data from the IMvigor210 cohort. Data processing was performed using R language. For single-cell data analysis, the Seurat pipeline was applied to conduct quality control, normalization, dimensionality reduction and cell annotation. Differential expression analysis, gene correlation analysis (Pearson correlation) and survival analysis (Kaplan-Meier method with Log-rank test) were carried out based on bulk expression profile data. The relationships between the expression levels of *SETD8* (gene symbol: KMT5A) and MCM7 and clinicopathological characteristics were analyzed using nonparametric tests. In the IMvigor210 cohort, the chi-square test was used to compare the differences in immunotherapy response rates between the gene high-expression and low-expression groups.

### 2.2 Cell culture

GES-1 and gastric carcinoma cell lines, including GSU, Hs 746.T, LMSU, MKN-74 and SNU-484, were obtained from the ATCC cell bank (https://www.atcc.org/). All cells were cultured in RPMI-1640 medium (Cytiva, USA) supplemented with 10% fetal bovine serum (FBS; Clark Bioscience, USA) and 1% penicillin-streptomycin (HyClone, USA), under standard condition: 37°C, 5% $CO_2$ and 95% air humidified atmosphere. All cell lines were authenticated by short tandem repeat (STR) profiling and tested negative for mycoplasma contamination using a PCR-based detection method prior to use.

### 2.3 Quantitative real-time PCR (qRT-PCR)

Total RNA was extracted using Trizol reagent (Invitrogen, Carlsbad, USA), followed by reverse transcription into cDNA with the PrimeScript RT kit (TaKaRa, Japan) according to the manufacturer's protocol. Target gene expression was quantified by quantitative PCR (qPCR) using an ABI 7900HT Real-Time PCR system (Applied Biosystems, Foster City, USA). The threshold cycle (Ct) values for genes of interest were determined based on amplification curves plotting fluorescenceintensity against PCR cycle number. The ΔCt values were calculated as the difference in Ct values between control and experimental groups. Using β-actin as the endogenous control, relative fold-changes in target gene expression were analyzed via the 2^(-ΔΔCt) method. All reactions were performed in triplicate. All primers were synthesized by General Biosystems, with the following primer sequences in Table 1.

Table 1 Sequences of primers used in the study

| Gene name | Forward primer (5'→3') | Reverse primer(3'→5') |
|---|---|---|
| ***SETD8*** | ATGGCAAAGGCAGGGGTGTGATTG | GCGATGAGGATGAGGTGAGGTACG |
| ***MCM7*** | CCTACCAGCCGATCCAGTCT | CCTCCTGAGCGGTTGGTTT |
| **β-actin** | ATCATGTTTGAGACCTTCAA | CATCTCTTGCTCGAAGTCCA |

### 2.4 CCK-8

Cell proliferation was determined using a CCK8 assay kit (Dojindo, Japan). Briefly, GSU cells were pre-seeded at $1 \times 10^3$ cells/well in 96-well plates 24 h prior to analysis. Following daily supplementation with 100 μL medium containing 10 μL CCK8 reagent, plates were incubated for 2 h

and absorbance at 450 nm recorded using a Multi-Mode Microplate Reader (Biotek, USA).

**2.5 Apoptosis analysis**

Apoptosis was quantified by flow cytometry using Annexin V-FITC/PI dual staining (Transgen, China). Treated cells underwent trypsinization, centrifugation (300 × g, 5 min), and two ice-cold PBS washes. Cell pellets were resuspended in 300 µL binding buffer with 5 µL Annexin V-FITC (15 min, dark). Prior to the flow cytometer (BD FACSCanto™ II) acquisition, 5 µL PI and 200 µL binding buffer were added.

**2.6 Western blot (WB) analysis**

Cells were washed with ice-cold PBS and lysed in buffer containing 1% PMSF. Following centrifugation at 14,000 × g for 5 min at 4°C, supernatants were collected for protein quantification using a BCA Protein Assay Kit. Equal protein aliquots (30 µg) underwent SDS-PAGE separation and subsequently wet-transfer onto polyvinylidene difluoride (PVDF) membranes. Post-blocking with bovine serum albumin (BSA), the membranes received three 5 min Tris-buffered saline and 0.1% Tween® 20 (TBST) washes before incubation at 4°C with the following primary antibodies: anti-N-cadherin (1:1000, Proteintech), anti-E-cadherin (1:2000, Proteintech), anti-vimentin (1:2000, Proteintech), anti-snail (1:1000, CST), anti-SETD8 (1:1000, CST) and anti-MCM7 (1:1000, CST). After washing thrice with TBST for 5 min, HRP-conjugated secondary antibodies (1: 30,000 in TBST) were applied for 2 h at room temperature. Immunoreactive bands were detected by enhanced chemiluminescence and quantified using Image-Pro Plus version 6.0 software (Media Cybernetics), with GAPDH normalization.

**2.7 Immunofluorescence**

Cells fixed on coverslips were blocked with 10% goat serum for 1 h at 37°C, followed by overnight incubation at 4°C with primary antibodies: anti-N-cadherin (1:100, CST, USA) and anti-E-cadherin (1:100, Abcam, UK). Subsequent incubation with FITC-conjugated or TRITC conjugated secondary antibodies proceeded for 45 min, with nuclear counterstaining using DAPI (Beyotime) for

3min. Finally, images were performed on a confocal fluorescence microscope (Nikon, Japan), and fluorescence intensity was quantified via Image J software 2.1 (Bethesda, MD, USA).

**2.8 Transwell**

GC cells were enumerated, resuspended in 150 µL serum-free medium, and plated into the upper chamber of a Transwell chamber (Corning, USA) with 8 µm pore sizes. The lower chamber was filled with 650 µL of medium containing 20% FBS. For invasion assay, matrigel-coated inserts (BD Biosciences, USA) were identically processed. Following 24 h incubation, the cells in the chambers were washed twice with PBS, fixed with 4% paraformaldehyde and stained with 0.1% crystal violet. Following natural air-drying, samples were observed and photographed under a Leica microscope (DMI1; Wetzlar, Germany).

**2.9 Wound healing assay**

In wound healing assays, GC cells were grown to 100% confluence in 6-well plates. Scratches were generated in monolayers using a 100 µL pipette tip, followed by serum-free medium replacement. Identical fields were documented at 0 h and 24 h post-scratching.

**2.10 Sphere formation assay**

Pretreated cells at 85% confluency underwent PBS washing, trypsin digestion, and serum-free medium resuspension prior to counting. The sphere formation medium consisted of DMEM/F12 basal medium supplemented with 20 ng/mL human recombinant EGF, 20 ng/mL human recombinant bFGF, 1× B-27 Supplement, and 1× penicillin-streptomycin. Triplicate seeding in Corning Ultra Low Attachment plates at $1\times10^4$ cells/well preceded 7-day incubation under standard culture conditions. Half of the medium was carefully replaced with fresh sphere formation medium every 3 days. Bright-field microscopy documented tumor spheres (defined as spherical cell aggregates with a diameter ≥ 50 µm), with ImageJ-based quantification of sphere number and size.

### 2.11 Detection of Stem Cell Markers

Cells were collected, digested with trypsin to prepare a single-cell suspension, and washed with PBS. A total of $1\times10^6$ cells were resuspended in 100 µL staining buffer, followed by the addition of anti-human CD44-FITC and anti-human CD24-PE antibodies (1:100 dilution), and incubation at 4 °C for 30 minutes in the dark. After incubation, the cells were washed and resuspended in 300 µL staining buffer. Detection was performed on a BD FACSCanto™ II flow cytometer with gating set according to isotype controls. The proportion of $CD44^+CD24^-$ cell population was analyzed using FlowJo software (v10.8).

### 2.12 ChIP-qPCR analysis

ChIP was conducted with Cell Signaling Technology kit (#9003) per manufacturer's protocol and published methods (36358786), utilizing 200-500 bp DNA fragments. Sheared chromatin received anti-H4K20me1 antibody (Abcam #9051; 1:50 dilution, Lot GR288167-1) for 16 h incubation at 4°C.

### 2.13 Statistical analysis

All experiments included more than 3 independent replicates. Statistical processing utilized SPSS 27.0 and GraphPad Prism 9.3, with continuous variables expressed as mean ± SD. Intergroup comparisons employed Student's t-test or ANOVA, significance denoted as: *P < 0.05, n.s. (no significant).

## 3. Results

### 3.1 Upregulation of *SETD8* in GC

We utilized TIMER2.0 to analyze the differential expression of *SETD8* between normal and tumor tissues across various cancer types (Figure 1A). This indicated that *SETD8* expression was significantly elevated in multiple cancers, including breast cancer, cholangiocarcinoma, colon adenocarcinoma, esophageal cancer, head and neck squamous cell carcinoma, kidney cancer, liver

cancer, lung cancer, and gastric adenocarcinoma (a subtype of GC).

Additionally, validation using data from TCGA confirmed that *SETD8* expression was upregulated in GC (Figure 1B). Survival analysis revealed a significant positive correlation between high expression of *SETD8* and poor prognosis (Figure 1C). Receiver operating characteristic (ROC) curve analysis assessed *SETD8*'s diagnostic efficacy for gastric cancer, generating an area under the curve (AUC) of 0.699 which denotes moderate diagnostic accuracy (Figure 1D). Furthermore, we examined *SETD8* expression in cell lines and found that its mRNA levels were significantly higher in GC cell lines (GSU, Hs 746.T, LMSU, MKN-74 and SNU-484) compared to GES-1 (Figure 1E). These findings collectively suggest that *SETD8* is upregulated in GC, highlighting its potential role in tumor progression.

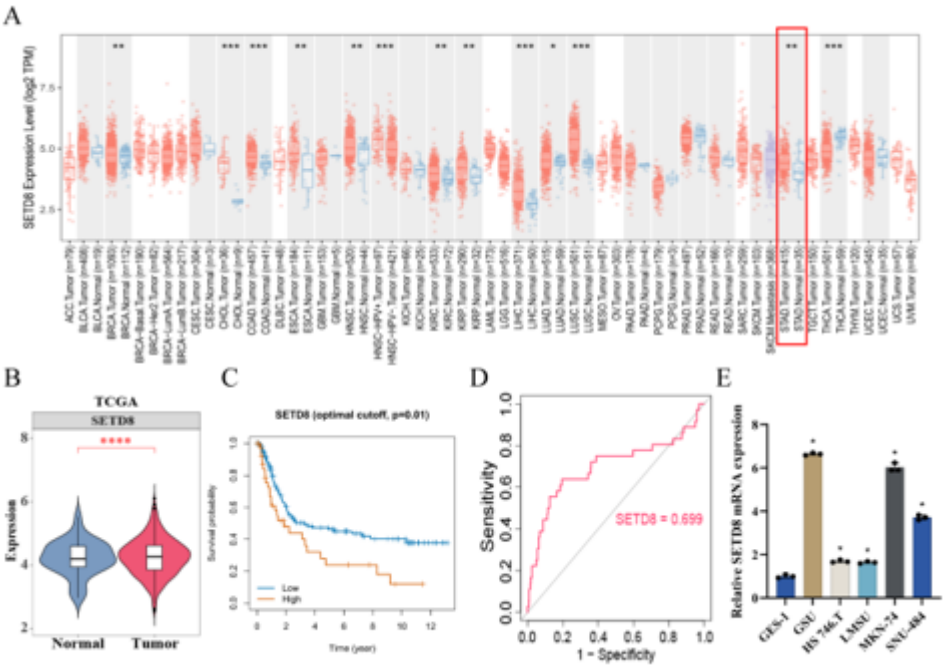


Figure 1. Upregulation of *SETD8* Expression in GC. (A) TIMER2.0 analysis of the TCGA database shows *SETD8* expression across various cancer types. (B) TCGA database analysis indicates that *SETD8* expression is significantly elevated in GC. (C) Kaplan-Meier survival analysis showing *SETD8* expression levels and Overall Survival in GC patients. (D) ROC analysis and AUC measurement demonstrate the diagnostic potential of *SETD8* in GC, with an AUC value of 0.699. (E) qRT-PCR

analysis reveals that *SETD8* expression is higher in GC cell lines (GSU, Hs 746.T, LMSU, MKN-74 and SNU-484) compared to GES-1. Data are from three independent experiments (n=3), presented as mean ± SD.

### 3.2 *SETD8* Promotes GC Progression

The above findings indicate that elevated *SETD8* expression correlates in GC. Previous studies have shown that *SETD8* expression is relatively high in GSU and MKN74 cells among GC cell lines (Figure 1E), leading us to select GSU and MKN74 cells for further functional experiments. WB analysis confirmed the efficient knockdown of SETD8 protein in both cell lines (Figure 2A). Consistently, RT-qPCR analysis revealed that the mRNA expression of *SETD8* was significantly decreased (Figure 2B). Functionally, *SETD8* knockdown significantly reduced the viability of GC cells in a time-dependent manner, with viability progressively declining and plateauing after 48 hours (Figure 2C; Figure S1A). Furthermore, *SETD8* depletion markedly increased cellular apoptosis. *SETD8* knockdown induced a 3-fold increase in apoptotic rate relative to the Control group (Figure 2D; Figure S1B). Additionally, transwell (Figure 2E; Figure S1C) and wound healing assays (Figure 2F; Figure S1D) revealed that *SETD8* knockdown markedly impaired the invasive and migratory abilities of GC cells. *SETD8* knockdown halved both invasion and migration rates in GC cells compared to the Control group. These results indicate that SETD8 plays a pivotal role in promoting GC progression.

Revista Española de Enfermedades Digestivas
The Spanish Journal of Gastroenterology

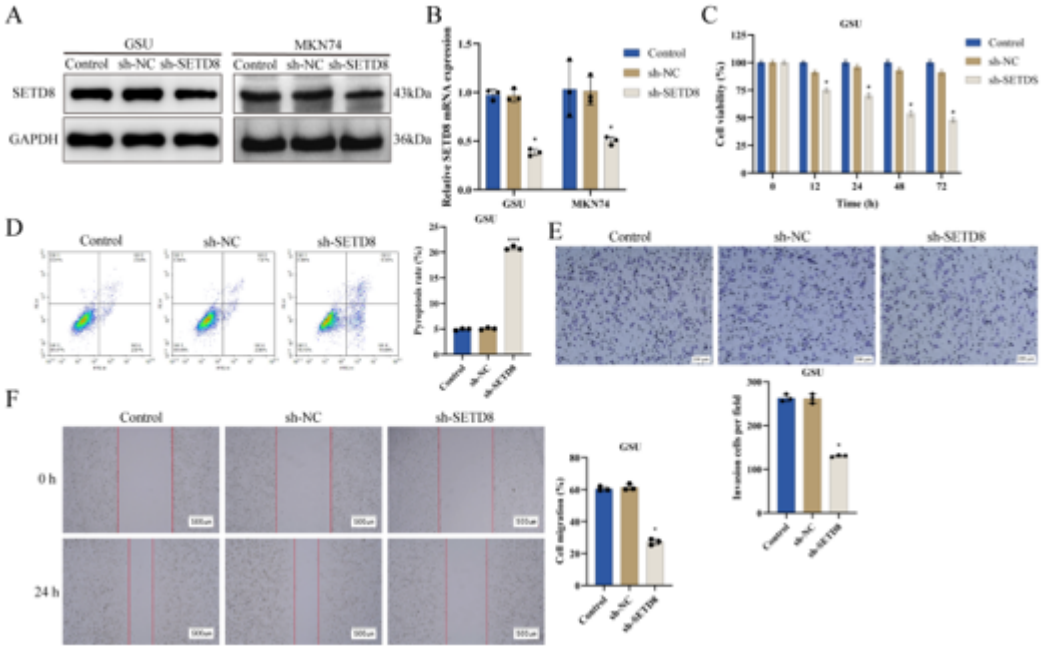


Figure 2. *SETD8* Promotes GC Progression. (A) WB of SETD8 and MCM7 protein expression levels. (B) qRT-PCR of *SETD8* and *MCM7* mRNA expression levels. (C) CCK-8 assay assessing cell viability. (D) Flow cytometry analysis evaluating cell apoptosis. (E) Transwell invasion assay measuring the invasive capacity of GSU cells. (F) Wound healing assay assessing cell migration ability. Data are from three independent experiments (n=3), presented as mean ± SD.

### 3.3 *SETD8* Regulates *MCM7* Expression via H4K20me1 to Promote EMT in GC

To elucidate the downstream mechanisms by which SETD8 drives GC progression, we examined the correlation between *SETD8* and *MCM7*. Analysis of GC patient data revealed a positive correlation between *SETD8* and *MCM7* expression (Figure 3A). Previous studies have reported that *MCM7* is highly expressed in GC (28540486, 24647462), which was corroborated by our validation using TCGA-GC datasets (Figure 3B). The survival analysis indicates that high expression of *MCM7* is positively correlated with poor prognosis (Figure 3C). Further validation in cell lines showed that *MCM7* mRNA levels were significantly higher in GC cell lines (GSU, Hs 746.T, LMSU, MKN-74 and SNU-484) than in normal gastric epithelial cells (GES-1) (Figure 3D). Notably,

*SETD8* knockdown in GUS cells resulted in a significant reduction in *MCM7* expression at both the protein and mRNA levels (Figure 3E,F; Figure S2A, B), suggesting that *MCM7* is a downstream effector of SETD8 in GC.

SETD8 is a histone methyltransferase that specifically catalyzes H4K20me1, a modification known to regulate transcription and promote cell proliferation and migration (35351142). To determine whether SETD8 regulates *MCM7* through H4K20 methylation, we conducted WB analysis, which revealed that *SETD8* knockdown led to decreased H4K20me1 levels. A similar reduction was observed upon treatment with UNC0379, a histone methyltransferase inhibitor (Figure 3E). Consistently, qRT-PCR analysis showed that both *SETD8* knockdown and UNC0379 treatment significantly downregulated the mRNA expression of *MCM7* (Figure 3F), linking *SETD8*'s catalytic activity to *MCM7* transcription.

To directly investigate whether SETD8 binds to the *MCM7* promoter and deposits H4K20me1, we performed ChIP-qPCR analysis. The results demonstrated significant enrichment of H4K20me1 at the *MCM7* promoter region in control cells, which was substantially diminished upon *SETD8* knockdown (Figure 3G; Figure S2C), indicating that SETD8 catalytic activity is required for this modification. However, ChIP-qPCR conducted with an anti-SETD8 antibody revealed no significant enrichment of SETD8 at the *MCM7* promoter compared to the IgG control (Figure 3H; Figure S2D). This suggests that SETD8 may not stably and directly bind to the *MCM7* promoter, implying a non-canonical regulatory mechanism. To functionally validate that SETD8-mediated H4K20me1 modification enhances transcription, we conducted a luciferase reporter assay. The activity of the *MCM7* promoter-driven luciferase was significantly reduced following *SETD8* knockdown (Figure 3I; Figure S2E), confirming that SETD8 positively regulates *MCM7* promoter activity.

EMT is a key mechanism driving cancer metastasis (37758242), we next examined whether the SETD8/H4K20me1/*MCM7* axis influences this process. WB and qRT-PCR analysis confirmed that *SETD8* knockdown or UNC0379 treatment significantly increased E-cadherin expression while reducing Snail, N-cadherin and Vimentin levels (Figure 3J, K; Figure S2F, G).

Collectively, these findings suggest that SETD8 is recruited to the *MCM7* promoter, where it catalyzes H4K20me1 modification to enhance *MCM7* transcription, thereby driving the EMT program and promoting GC progression.

Revista Española de Enfermedades Digestivas
The Spanish Journal of Gastroenterology

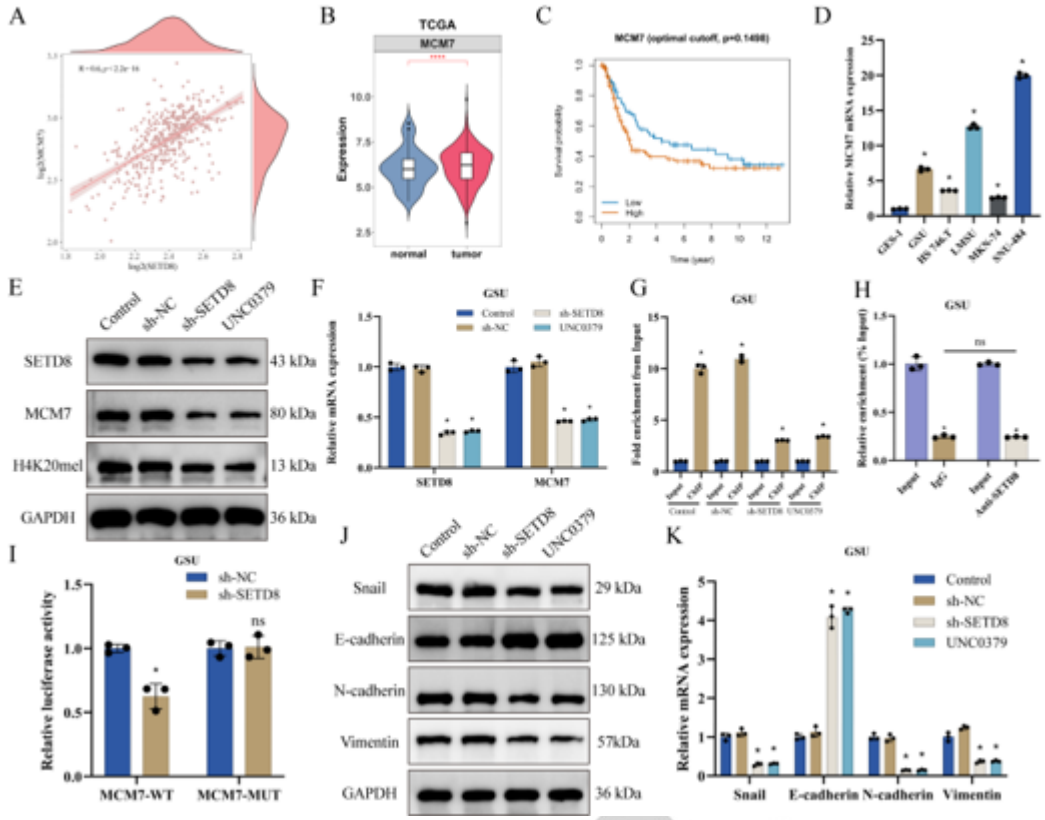


Figure 3. *SETD8* Facilitates EMT in GC by Regulating *MCM7* Expression through H4K20me1. (A) Correlation analysis indicates a positive association between *SETD8* and *MCM7* expression in GC patients. (B) TCGA database validation confirms that *MCM7* is significantly overexpressed in GC. (C) Kaplan-Meier survival analysis showing *SETD8* expression levels and Overall Survival in GC patients. (D) qRT-PCR analysis shows higher *MCM7* expression in GC cell lines (GSU, Hs 746.T, LMSU, MKN-74 and SNU-484) compared to GES-1. (E) WB analysis of SETD8, MCM7 and H4K20me1 protein expression levels. (F) qRT-PCR analysis of *SETD8*, *MCM7* and H4K20me1 mRNA expression levels. (G) ChIP-qPCR assay evaluating H4K20me1 enrichment at the *MCM7* promoter region. (H) ChIP-qPCR assay evaluating SETD8 enrichment at the *MCM7* promoter region. (I) Luciferase reporter assay assessing the activity of the *MCM7* promoter upon *SETD8* knockdown. (J) WB analysis of EMT-associated proteins (Snail, E-cadherin, N-cadherin, Vimentin) expression levels. (K) qRT-PCR analysis of EMT-associated proteins (Snail, E-cadherin, N-cadherin, Vimentin) mRNA expression levels. Data are from three independent experiments (n=3), presented as mean ± SD. ChIP-qPCR: Chromatin

immunoprecipitation followed by qPCR. qRT-PCR: Quantitative real-time polymerase chain reaction. EMT: Epithelial-mesenchymal transition.

To further investigate the expression patterns and potential biological implications of *SETD8* and *MCM7* in gastric cancer, we performed a series of analyses based on the gastric cancer single-cell transcriptome dataset (GSE183904) and the GEO dataset (GSE15459). Cell type annotation of single-cell data from gastric cancer tissues (GSE183904) revealed that the tissues mainly contained multiple cell types including epithelial cells, T cells, endothelial cells and fibroblasts (Figure 4A-C). In tissue samples from gastric cancer patients and healthy controls, the expressions of *SETD8* (gene symbol: *KMT5A*) and *MCM7* were both upregulated (Figure 4D). UMAP visualization at the single-cell level further confirmed that *SETD8* (*KMT5A*) and *MCM7* were highly co-expressed in gastric cancer tissues, particularly in the proliferative epithelial cell subset (Figure 4E). Analysis of immunotherapy data from the IMvigor210 cohort showed that tumors with high *SETD8* (*KMT5A*) or *MCM7* expression exhibited relatively high immune response activity (Figure 4F). Correlation analysis indicated that the expression levels of both *SETD8* (*KMT5A*) and *MCM7* were significantly positively correlated with the expression of Snail (*SNAI1*), a core transcription factor of EMT (Figure 4G). Additionally, in the dataset (GSE15459), high expressions of *SETD8* (*KMT5A*) and *MCM7* were significantly associated with age, gender, advanced T stage and advanced clinical stage in gastric cancer patients (Figure 4H, I). These complementary results from independent datasets further validated and extended the aforementioned findings at the single-cell resolution and clinical correlation levels, collectively supporting the conclusion that *SETD8* and *MCM7* are synergistically highly expressed in gastric cancer and participate in the malignant progression of the disease.

Revista Española de Enfermedades Digestivas
The Spanish Journal of Gastroenterology

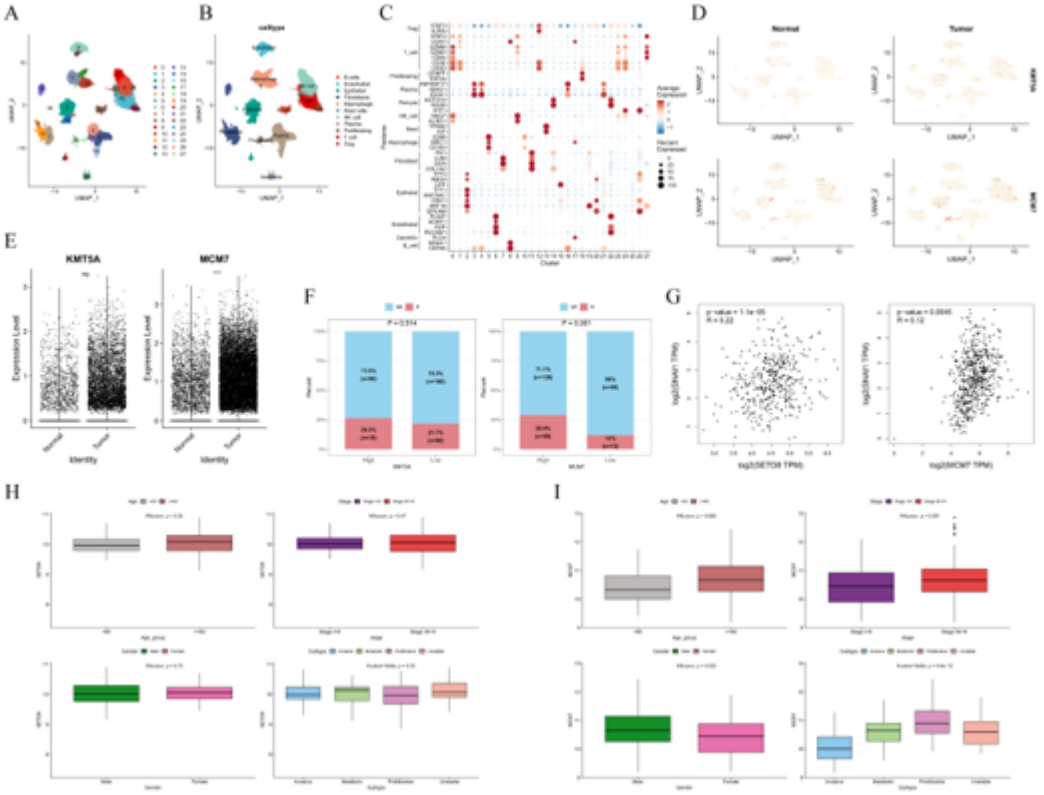


Figure 4. Expression Patterns and Clinical Correlations of *SETD8* and *MCM7* in GC. (A-C) Cell type annotation of single-cell sequencing data from gastric cancer tissues (GSE183904). (D) Expression trends of *SETD8* (gene symbol: *KMT5A*) and MCM7 in tissue samples from gastric cancer patients and healthy controls. (E) UMAP visualization at the single-cell level showing the co-expression pattern of *SETD8* (*KMT5A*) and *MCM7* in gastric cancer tissues. (F) Analysis of immune response activity based on immunotherapy data from the IMvigor210 cohort. (G) Correlation analysis between the expression levels of *SETD8* (*KMT5A*)/*MCM7* and Snail (*SNAI1*), a core transcription factor of EMT. (H-I) Correlation analysis of the high expression of *SETD8* (*KMT5A*) and *MCM7* with age, gender, T stage and clinical stage in gastric cancer patients from the dataset (GSE15459).

### 3.4 *MCM7* Overexpression Reverses *SETD8* Knockdown-Mediated Suppression of EMT and GC Progression

To independently establish the tumor-promoting function of *MCM7*, we conducted gain-of-function studies in GSU cells. Overexpression of *MCM7* was confirmed at both protein and mRNA

levels (Figure 5A, B). Functionally, *MCM7* overexpression significantly enhanced cell proliferation (Figure 5C), migration (Figure 5D), and invasion (Figure 5E). At the molecular level, *MCM7* overexpression robustly induced EMT, as demonstrated by decreased E-cadherin and increased Snail, N-cadherin, and Vimentin expression, evidenced by both WB and qRT-PCR analyses (Figure 5F, G). These data conclusively demonstrate that MCM7 is sufficient to drive malignant phenotypes and EMT in GC cells, solidifying its essential role as the key downstream effector of SETD8.

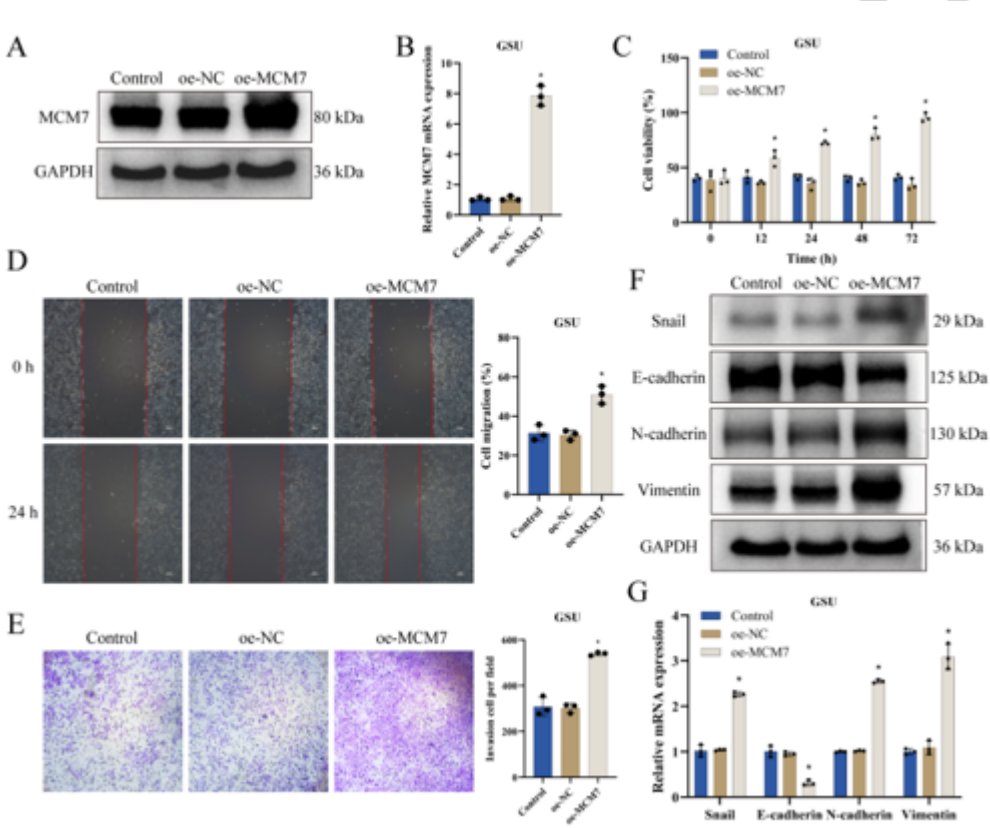


Figure 5. *MCM7* overexpression promotes GC Progression. (A) WB analysis confirming MCM7 protein overexpression. (B) qRT-PCR analysis confirming *MCM7* mRNA overexpression. (C) CCK-8 assay assessing cell proliferation upon *MCM7* overexpression. (D) Wound healing assessing cell migration ability. (E) Transwell invasion assay showing invasive capacity. (F) WB analysis of EMT-associated proteins (Snail, E-cadherin, N-cadherin, Vimentin) expression levels. (G) qRT-PCR analysis of EMT-associated proteins (Snail, E-cadherin, N-cadherin, Vimentin) mRNA expression levels. Data are from three independent experiments (n=3), presented as mean ± SD.

Revista Española de Enfermedades Digestivas
The Spanish Journal of Gastroenterology

To further directly test whether MCM7 is the critical functional downstream target of *SETD8*, we performed rescue experiments by overexpressing *MCM7* in the context of *SETD8* knockdown. First, WB analysis confirmed that the decreased MCM7 protein level resulting from *SETD8* knockdown was effectively restored by *MCM7* overexpression (Figure 6A; Figure S3A). Subsequently, qRT-PCR verified the successful reconstitution of *MCM7* at the mRNA level (Figure 6B; Figure S3B). Rescue experiments demonstrated that *MCM7* overexpression reversed the effects of *SETD8* knockdown, restoring the expression of EMT markers: the elevated E-cadherin levels observed in *SETD8*-knockdown cells were reduced, while N-cadherin levels were restored (Figure 6C; Figure S3C). Additionally, tumor sphere formation assays showed that *SETD8* knockdown led to impaired sphere-forming capacity, which was reversed by *MCM7* overexpression. Quantitative analysis revealed a 60% reduction in tumor sphere formation upon *SETD8* knockdown compared to the Control group. *MCM7* overexpression rescued this suppression, restoring sphere-forming capacity (Figure 6D). Transwell assays demonstrated that the inhibitory effect of SETD8 knockdown on GC cell invasion was also rescued by MCM7 overexpression (Figure 6E). Similarly, in wound healing assays, the impaired migration ability of *SETD8*-knockdown cells was restored by *MCM7* overexpression (Figure 6F). Collectively, these rescue experiments demonstrate that the pro-tumorigenic functions of *SETD8* are largely mediated through *MCM7*, establishing MCM7 as an essential downstream effector in the *SETD8*-driven GC progression pathway.

Revista Española de Enfermedades Digestivas
The Spanish Journal of Gastroenterology

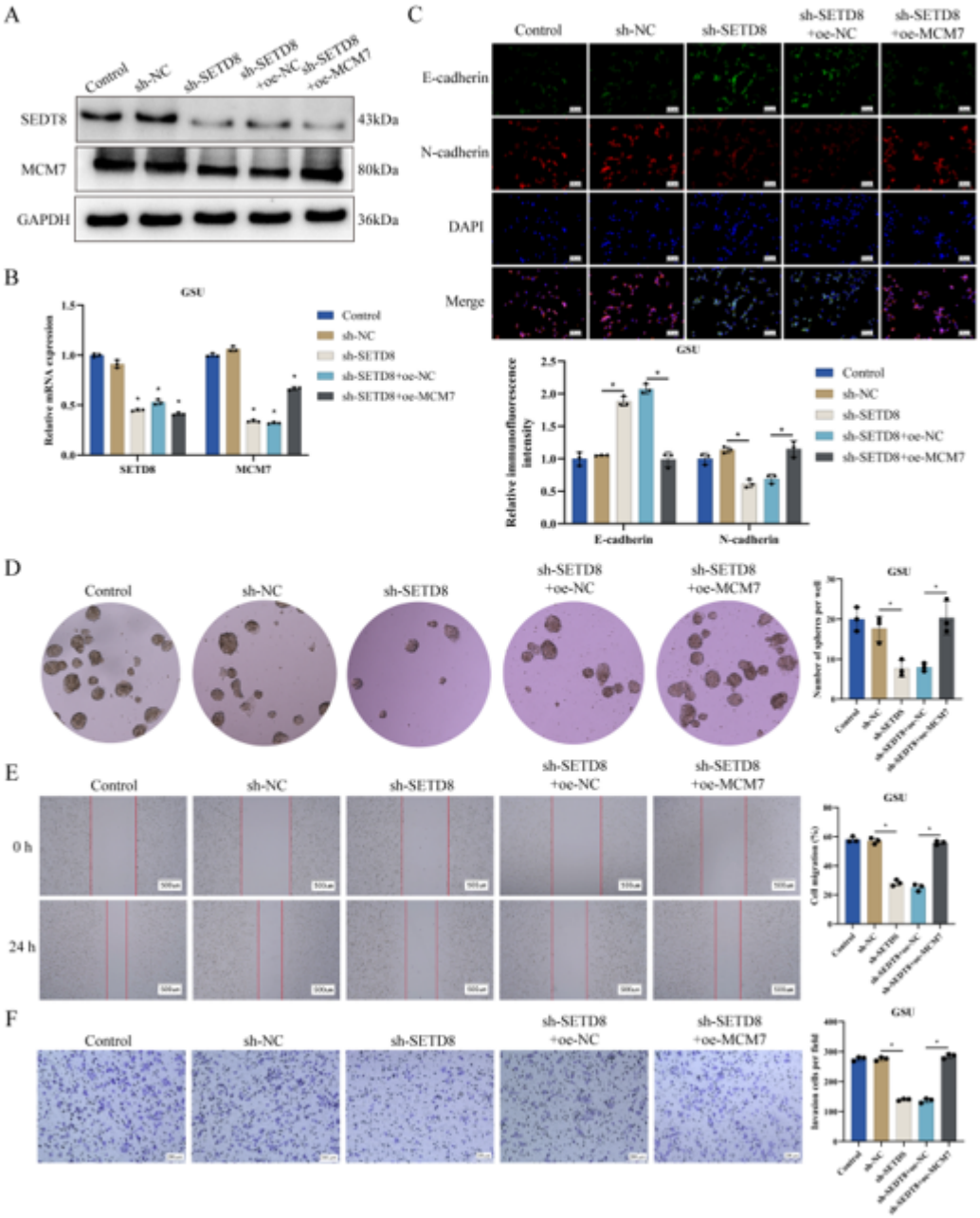


Figure 6. *MCM7* Overexpression Reverses *SETD8* Knockdown-Induced EMT Suppression and Restores GC Progression. (A) WB analysis of MCM7 protein expression levels. (B) qRT-PCR analysis of *SETD8* and *MCM7* mRNA expression levels. (C) Immunofluorescence staining of E-cadherin and N-cadherin. (D) Tumorsphere formation assay evaluating the stem-like potential of GC cells. (E) Transwell invasion assay measuring cell invasiveness. (F) Wound healing assay assessing cell migration ability. Data are from three independent experiments (n=3), presented as mean ± SD.

Revista Española de Enfermedades Digestivas
The Spanish Journal of Gastroenterology

To further investigate the impact of the *SETD8-MCM7* axis on cancer stem-like properties, we assessed sphere-forming capacity and stemness marker expression. First, serial passaging of tumor spheres revealed that *SETD8* knockdown significantly impaired the self-renewal ability of GC cells, as evidenced by reduced formation of secondary and tertiary spheres at 7 and 14 days, respectively. This defect was effectively rescued by *MCM7* overexpression (Figure 7A; Figure S3D). Consistently, flow cytometry analysis demonstrated that *SETD8* knockdown decreased the proportion of cells with the stem cell surface marker profile ($CD44^+CD24^-$), while *MCM7* overexpression restored this population (Figure 7B; Figure S3E). At the transcriptional level, the mRNA expression of key stemness-associated transcription factors (*NANOG*, *SOX2*, *OCT4*, and *KLF4*) was downregulated upon *SETD8* knockdown and was markedly recovered by *MCM7* reconstitution (Figure 7C; Figure S3F). Together, these data indicate that the *SETD8-MCM7* axis is crucial for maintaining the stem-like properties of GC cells, providing a mechanistic link between epigenetic regulation and cancer stemness.

Revista Española de Enfermedades Digestivas
The Spanish Journal of Gastroenterology

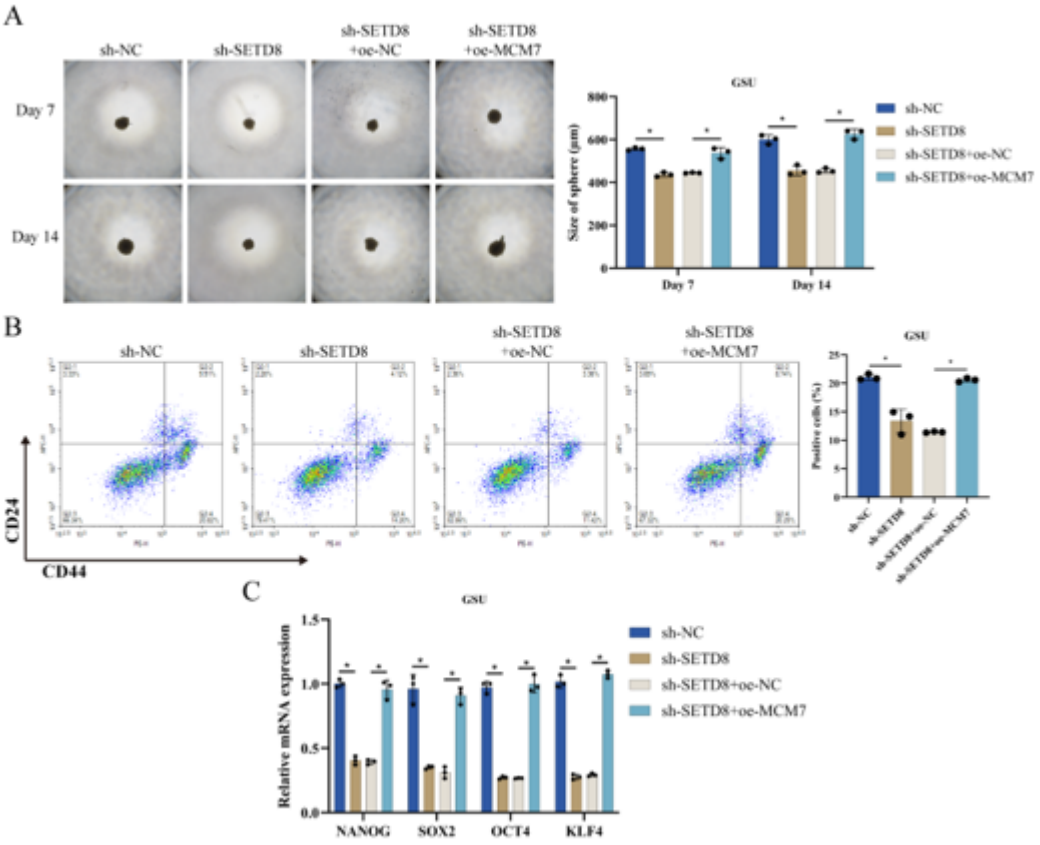


Figure 7. The *SETD8-MCM7* axis maintains cancer stem-like properties in GC cells. (A) Serial tumorsphere formation assay showing primary, secondary, and tertiary spheres. (B) Flow cytometry analysis for the $CD44^{+}CD24^{-}$ cell population. (C) qRT-PCR analysis of stemness-associated transcription factors (*NANOG*, *SOX2*, *OCT4*, *KLF4*). Data are from three independent experiments (n=3), presented as mean ± SD.

## 4. Discussion

This study provides novel insights into the role of the histone methyltransferase SETD8 in gastric cancer (GC) progression. Using integrated bioinformatic and in vitro approaches, we demonstrate that *SETD8* is upregulated in GC and that its knockdown suppresses malignant phenotypes, including proliferation, migration, invasion, and EMT. Furthermore, we identify *MCM7* as a key downstream mediator of SETD8, whose overexpression partially rescues the inhibitory effects of SETD8 depletion. These findings suggest that the *SETD8*/*MCM7* axis contributes to GC

aggressiveness, highlighting its potential as a therapeutic target.

Our observations align with prior reports indicating oncogenic functions of SETD8 in various cancers, such as breast and endometrial carcinomas, where it promotes tumor progression via H4K20me1-mediated transcriptional regulation [9-11]. Our findings are consistent with these observations and further suggest that SETD8 may exert its function through similar mechanisms in gastric cancer. Notably, *SETD8* expression is positively correlated with EMT-related genes, such as Snail and Vimentin, further supporting its role in promoting metastasis through EMT [9, 10]. However, the differential expression of *SETD8* across GC molecular subtypes (e.g., EBV-positive, genomically unstable subtypes) and its association with therapeutic resistance warrant further investigation. Rescue experiments demonstrated that *MCM7* overexpression effectively reverses the suppressive effects of *SETD8* knockdown on EMT and cellular invasion, confirming that MCM7 is a critical downstream effector of SETD8. MCM7 may promote EMT progression by activating the β-catenin signaling pathway, leading to the upregulation of transcription factors such as Snail and Twist [20, 21]. However, the specific downstream signaling pathways of MCM7 remain unclear and require further investigation using RNA sequencing or phosphoproteomics to identify potential effector molecules. Additionally, whether SETD8 regulates other EMT-related genes, such as *ZEB1* or *TWIST1*, via H4K20me1 modification remains to be validated to comprehensively elucidate its epigenetic regulatory network.

Histone modifications play a crucial role in gene expression regulation, and SETD8 is a specific methyltransferase for H4K20me1 [5]. ChIP-qPCR experiments in this study confirmed that *SETD8* knockdown or treatment with the methyltransferase inhibitor UNC0379 significantly reduces H4K20me1 enrichment at the *MCM7* promoter, correlating positively with *MCM7* expression. This finding is the first to directly link H4K20me1 modification with *MCM7* transcriptional activation, providing new insights into histone modification-mediated EMT regulation. Notably, H4K20me1 is generally associated with gene activation [22]. Our ChIP-qPCR experiments using an anti-SETD8 antibody revealed no significant enrichment of SETD8 at the *MCM7* promoter region. This indicates that SETD8 may not stably and directly bind to this promoter. This finding provides valuable insights, suggesting that SETD8-mediated regulation of *MCM7* likely occurs through a non-canonical mechanism that does not involve stable recruitment of SETD8 to the DNA sequence. However, whether SETD8 cooperates with other transcription factors to regulate *MCM7* promoter activity requires further exploration.

The clinical correlation analysis in this study further reinforces the pathological significance of the *SETD8*/*MCM7* axis. Beyond the TCGA cohort, our validation in the GEO datasets demonstrated that high expression of *SETD8* and *MCM7* is not only associated with tumorigenesis, but also significantly correlated with advanced T stage and clinical stage, suggesting that activation of this axis may serve as one of the drivers for enhanced aggressiveness and disease progression in gastric cancer. This finding is highly consistent with the results of in vitro experiments that the *SETD8*/*MCM7* axis promotes invasion, migration and stem cell phenotypes, providing a potential molecular explanation for the more aggressive clinical manifestations observed in patients with advanced gastric cancer. Notably, single-cell transcriptomic analysis revealed specific and high co-expression of *SETD8* and *MCM7* in the proliferative epithelial cell subset. This phenomenon implies that the axis may be preferentially activated in tumor cell subsets with robust proliferative and self-renewal potential, thereby being closely linked to tumor recurrence, metastasis and therapy resistance. Combined with the trend observed in the IMvigor210 immunotherapy cohort—that high expression of *SETD8* or *MCM7* may alter the status of the tumor immune microenvironment—future studies are warranted to further investigate whether targeting this axis can remodel the immune microenvironment and thus enhance the efficacy of immunotherapy.

Despite systematically elucidating the regulatory mechanism of the *SETD8*/*MCM7*/EMT axis, this study has several limitations: (1) The lack of in vivo validation necessitates the establishment of orthotopic GC xenograft models to assess the inhibitory effects of *SETD8* knockdown on tumor metastasis. (2) The relatively small clinical sample size requires expansion of the cohort and integration of multicenter data to validate the prognostic value of *SETD8* and *MCM7*. (3) The complexity of epigenetic regulation suggests that H4K20me1 may indirectly modulate gene expression through chromatin remodeling complexes, such as SWI/SNF, necessitating chromatin accessibility analyses using ATAC-seq. Furthermore, the development of small-molecule inhibitors targeting the *SETD8*/*MCM7* axis (e.g., a combination of UNC0379 with MCM7 monoclonal antibodies) may represent a novel therapeutic strategy for GC.

## 5. Conclusion

This study provides multidimensional experimental evidence demonstrating that SETD8 activates *MCM7* expression through an H4K20me1-dependent epigenetic mechanism, thereby

driving EMT and GC progression. Beyond elucidating molecular determinants of GC metastasis, these results provide a preclinical rationale for molecularly targeted interventions against the *SETD8*/*MCM7* axis. Subsequent investigations should prioritize clinical translation of this axis, employing SETD8 inhibitors or MCM7-directed therapeutics to enhance gastric cancer management. Assessing *SETD8* and *MCM7* expression levels in GC patients may serve as a valuable prognostic biomarker for risk stratification and personalized therapy. Additionally, given the involvement of SETD8 in multiple biological processes, its role in other signaling pathways and its impact on GC drug resistance warrant further investigation.

**Abbreviations**

GC: Gastric cancer

EMT: Epithelial-mesenchymal transition

qRT-PCR: Quantitative real-time polymerase chain reaction

ChIP-qPCR: Chromatin immunoprecipitation followed by qPCR

WB: Western blot

FBS: Fetal bovine serum

TCGA: The Cancer Genome Atlas

AUC: Area under the curve

ROC: Receiver operating characteristic

**Competing interests**

The authors declare that they have no potential conflicts of interest.

**Ethics approval and consent to participate**

Not applicable.

**Availability of data and materials**

Revista Española de Enfermedades Digestivas
The Spanish Journal of Gastroenterology

The data and materials in the current study are available from the corresponding author on reasonable request.

**Competing interests**

The authors have declared that no competing interest exists.

**Funding**

This work was supported by the "Health Management Excellent Youth Talent Project-Exploration of the Correlation between Hypertension and Extrahepatic Metastasis of Hepatocellular Carcinoma" from Shanghai Rehabilitation Medicine Association (Grant No. 2024JGYQ06) and the in-hospital research project "Clinical Study on Vitamin D Combined with EPO and Iron Agents in the Treatment of Cancer-Related Anemia" from Shanghai Pudong New Area People's Hospital (Grant No. E23-04).



Supplementary materials

Revista Española de Enfermedades Digestivas
The Spanish Journal of Gastroenterology

Supplementary materials

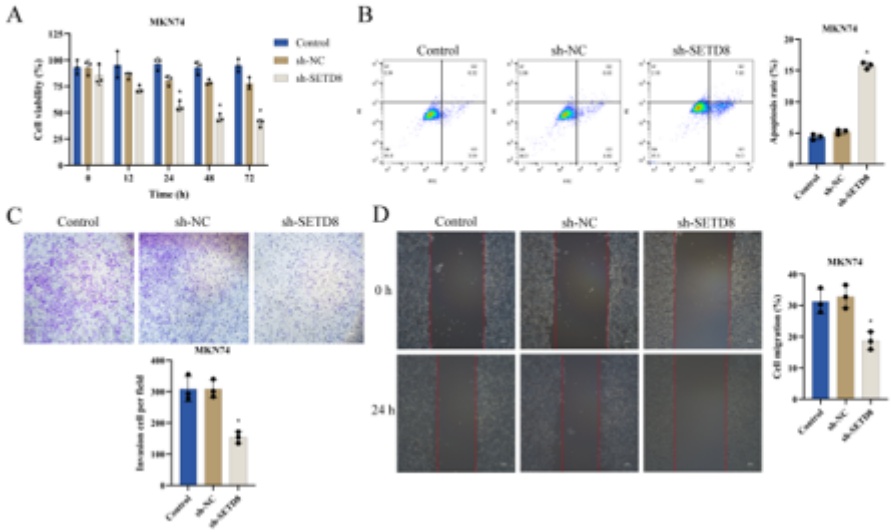


Figure S1. *SETD8* Promotes GC Progression. (A) CCK-8 assay assessing cell viability. (B) Flow cytometry analysis evaluating cell apoptosis. (C) Transwell invasion assay measuring the invasive capacity of GSU cells. (D) Wound healing assay assessing cell migration ability.

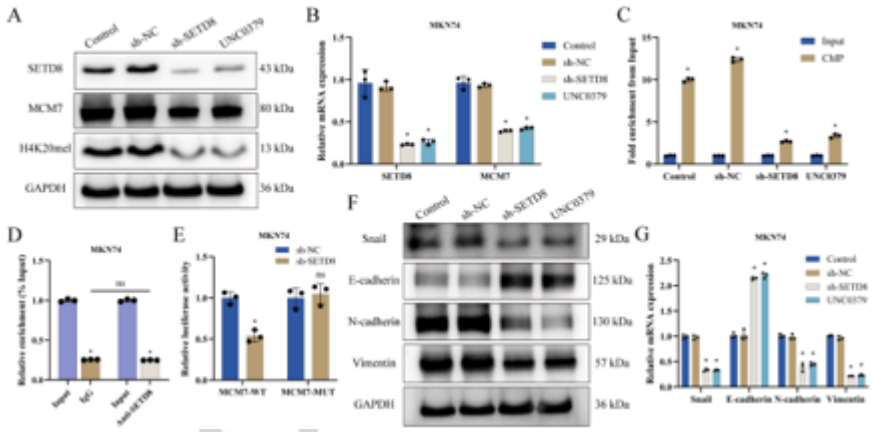


Figure S2. *SETD8* Facilitates EMT in GC by Regulating *MCM7* Expression through H4K20me1. (A) WB analysis of SETD8, MCM7 and H4K20me1 protein expression levels. (B) qRT-PCR analysis of *SETD8*, *MCM7* and H4K20me1 mRNA expression levels. (C) ChIP-qPCR assay evaluating H4K20me1 enrichment at the *MCM7* promoter region. (D) ChIP-qPCR assay evaluating SETD8 enrichment at the *MCM7* promoter region. (E) Luciferase reporter assay assessing the activity of the *MCM7* promoter upon *SETD8* knockdown. (F) WB analysis of EMT-associated proteins (Snail, E-cadherin, N-cadherin,

Vimentin) expression levels. (G) qRT-PCR analysis of EMT-associated proteins (Snail, E-cadherin, N-cadherin, Vimentin) mRNA expression levels.

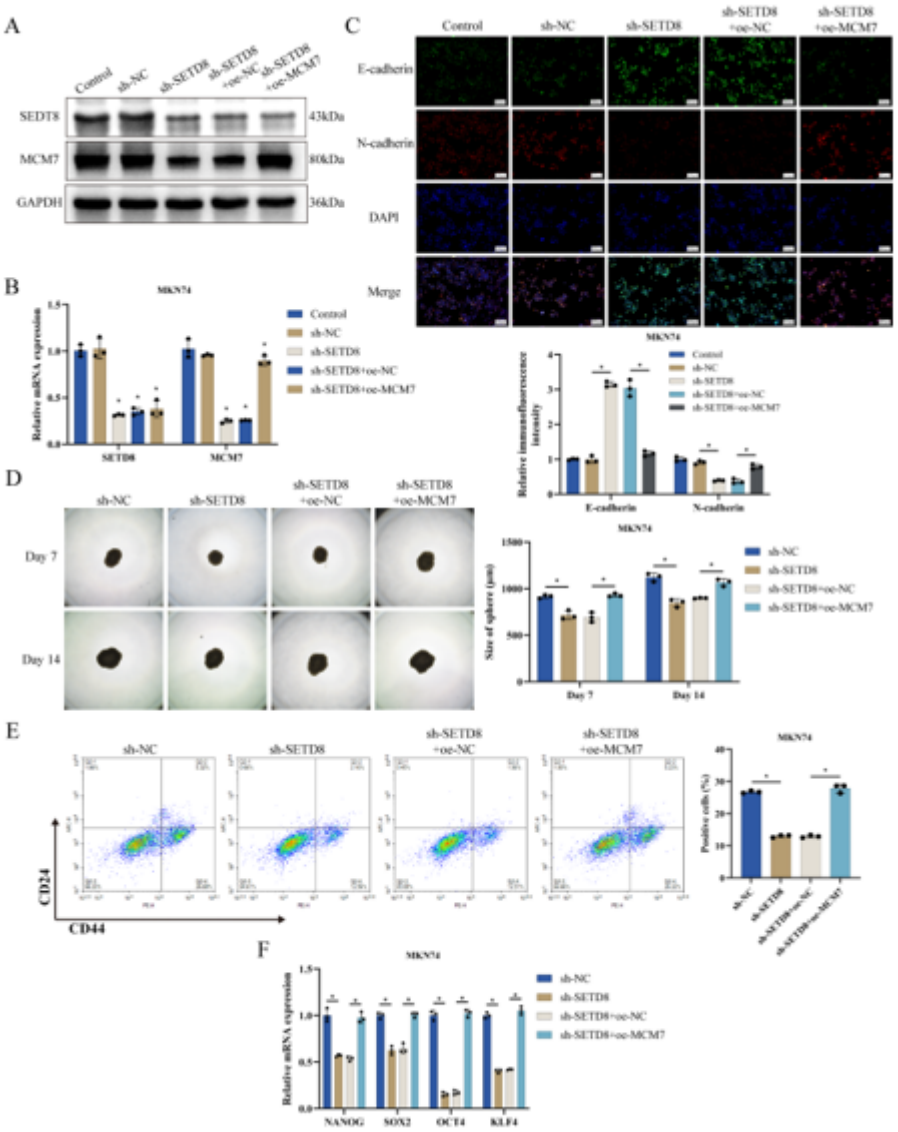


Figure S3. *MCM7* Overexpression Reverses *SETD8* Knockdown-Induced EMT Suppression and Restores GC Progression. (A) Western blot analysis of MCM7 protein expression levels. (B) qRT-PCR analysis of *SETD8* and *MCM7* mRNA expression levels. (C) Immunofluorescence staining of E-cadherin and N-cadherin. (D) Serial tumorsphere formation assay showing primary, secondary, and tertiary spheres. (E) Flow cytometry analysis for the CD44+CD24- cell population. (F) qRT-PCR analysis of stemness-associated transcription factors (NANOG, SOX2, OCT4, KLF4).

**References**

[1] W L Guan,Y He, R H Xu. Gastric cancer treatment: recent progress and future perspectives. J Hematol Oncol 2023;16: 57.

[2] W J Yang,H P Zhao,Y Yu et al. Updates on global epidemiology, risk and prognostic factors of gastric cancer. World J Gastroenterol 2023;29: 2452-2468.

[3] R Fontana,A Mestre-Farrera, J Yang. Update on Epithelial-Mesenchymal Plasticity in Cancer Progression. Annu Rev Pathol 2024;19: 133-156.

[4] D Li,L Xia,P Huang et al. Heterogeneity and plasticity of epithelial-mesenchymal transition (EMT) in cancer metastasis: Focusing on partial EMT and regulatory mechanisms. Cell Prolif 2023;56: e13423.

[5] L Xu,L Zhang,J Sun et al. Roles for the methyltransferase SETD8 in DNA damage repair. Clin Epigenetics 2022;14: 34.

[6] M Murga,G Lopez-Pernas,R Soliva et al. SETD8 inhibition targets cancer cells with increased rates of ribosome biogenesis. Cell Death Dis 2024;15: 694.

[7] Z Lu,Q Hu,Y Qin et al. SETD8 inhibits ferroptosis in pancreatic cancer by inhibiting the expression of RRAD. Cancer Cell Int 2023;23: 50.

[8] B Ke, K Ye. SETD8 promotes glycolysis in colorectal cancer via regulating HIF1α/HK2 axis. Tissue Cell 2023;82: 102065.

[9] M Liu,Y Shi,Q Hu et al. SETD8 induces stemness and epithelial-mesenchymal transition of pancreatic cancer cells by regulating ROR1 expression. Acta Biochim Biophys Sin (Shanghai) 2021;53: 1614-1624.

[10] R Huang,Y Yu,X Zong et al. Monomethyltransferase SETD8 regulates breast cancer metabolism via stabilizing hypoxia-inducible factor 1α. Cancer Lett 2017;390: 1-10.

[11] A Kukita,K Sone,S Kaneko et al. The Histone Methyltransferase SETD8 Regulates the Expression of Tumor Suppressor Genes via H4K20 Methylation and the p53 Signaling Pathway in Endometrial Cancer Cells. Cancers (Basel) 2022;14: 5367.

[12] S Mukherjee,S Das,N Sriram et al. In silico investigation of the role of vitamins in cancer therapy through inhibition of MCM7 oncoprotein. RSC Adv 2022;12: 31004-31015.

[13] Q Shi,G Xu,Y Jiang et al. Phospholipase PLCE1 Promotes Transcription and Phosphorylation of MCM7 to Drive Tumor Progression in Esophageal Cancer. Cancer Res 2024;84: 560-576.

[14] D Su. MCM7 affects the cisplatin resistance of liver cancer cells and the development of liver cancer by regulating the PI3K/Akt signaling pathway. Immunopharmacol Immunotoxicol 2022;44: 17-27.

[15] X Ke,B Xing,B Yu et al. IUGR disrupts the PPARγ-Setd8-H4K20me(1) and Wnt signaling pathways in the juvenile rat hippocampus. Int J Dev Neurosci 2014;38: 59-67.

[16] W Xue,L Yang,C Chen et al. Wnt/β-catenin-driven EMT regulation in human cancers. Cell Mol Life Sci 2024;81: 79.

[17] Y Jin,Y Xia,H Du et al. Super-enhancer-associated EEPD1 facilitates EMT-mediated metastasis by regulating the PI3K/AKT/mTOR pathway in gastric cancer. Biochem Biophys Res Commun 2023;689: 149188.

[18] L He,X Qian,P Ge et al. NOL6 Regulates the Proliferation and Apoptosis of Gastric Cancer Cells via Regulating TP53I3, CDK4 and MCM7 Expression. Front Oncol 2022;12: 708081.

[19] T G Selvan,P Gollapalli,S H S Kumar et al. Early diagnostic and prognostic biomarkers for gastric cancer: systems-level molecular basis of subsequent alterations in gastric mucosa from chronic atrophic gastritis to gastric cancer. J Genet Eng Biotechnol 2023;21: 86.

[20] Y Zhang,L Xu,P Wang et al. Phenotypic transition of tumor cells between epithelial- and mesenchymal-like state during adaptation to acidosis. Cell Cycle 2019;18: 1938-1947.

[21] J Mo,Z Gao,L Zheng et al. Targeting mitochondrial one-carbon enzyme MTHFD2 together with pemetrexed confers therapeutic advantages in lung adenocarcinoma. Cell Death Discov 2022;8: 307.

[22] X Lv,Z Han,H Chen et al. A positive role for polycomb in transcriptional regulation via H4K20me1. Cell Res 2016;26: 529-42.